Direct Measurement of the Mn(II) Hydration State in Metal Complexes and Metalloproteins through ^{17}O NMR Line Widths

Eric M. Gale, Jiang Zhu,[†] and Peter Caravan*

The Athinoula A. Martinos Center for Biomedical Imaging, Department of Radiology, Massachusetts General Hospital, Harvard Medical School, 149 Thirteenth Street, Suite 2301, Charlestown, Massachusetts 02129, United States

Ⓢ *Supporting Information*

ABSTRACT: Here we describe a simple method to estimate the inner-sphere hydration state of the Mn(II) ion in coordination complexes and metalloproteins. The line width of bulk $H_2^{17}O$ is measured in the presence and absence of Mn(II) as a function of temperature, and transverse ^{17}O relaxivities are calculated. It is demonstrated that the maximum ^{17}O relaxivity is directly proportional to the number of inner-sphere water ligands (q). Using a combination of literature data and experimental data for 12 Mn(II) complexes, we show that this method provides accurate estimates of q with an uncertainty of ± 0.2 water molecules. The method can be implemented on commercial NMR spectrometers working at fields of 7 T and higher. The hydration number can be obtained for micromolar Mn(II) concentrations. We show that the technique can be extended to metalloproteins or complex:protein interactions. For example, Mn(II) binds to the multimetal binding site A on human serum albumin with two inner-sphere water ligands that undergo rapid exchange (1.06×10^8 s^{-1} at 37 °C). The possibility of extending this technique to other metal ions such as Gd(III) is discussed.
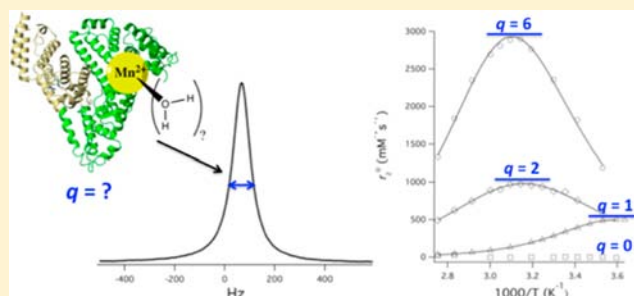
INTRODUCTION

The hydration state of metal ions in aqueous solution is fundamental to a variety of physical, chemical, and biological processes. It has been proposed that selectivity in ion transport across cellular membranes is driven by a topological control mechanism, where the thermodynamics of transport correlate directly to hydration number rather than affinity for ligand donors found within the transport channel.[1,2] Studies also suggest that the immediate solvation environment exerts direct control over the energetics and composition of the frontier molecular orbitals in reactive transition metal complexes.[3] Additionally, the solvation properties of a given ion can be reflective of macroscopic properties, and information regarding bulk environment can be extrapolated through probing this microscopic feature.[4−6] Although the hydration state of metal ions underlies essential physical and life processes, this fundamental property can be difficult to discern.

X-ray crystallography can provide high-resolution structural data of small complexes and macromolecules, but static structures obtained from crystalline samples do not always accurately describe solvent binding, equilibrium compositions, and environmentally triggered structural changes evidenced by solution spectroscopic techniques.[7−12] Additionally, this technique is limited by the need to obtain well-formed single crystals, which is not tenable for all samples. Extended X-ray absorbance fine structure (EXAFS) spectroscopy probes the primary coordination sphere of metal ions in solution[13−20] but cannot necessarily distinguish or quantify the number of water

ligands and requires access to a specialized facility with tunable synchrotron radiation. Solution neutron diffraction can determine the hydration state of ions in solution, but this technique also requires highly specialized instrumentation and very high (molar) concentrations.[21,22] At molar concentrations, intermolecular interactions become increasingly significant, resulting in changes in hydration state that do not reflect those relevant to physiological or catalytic processes.[23,24] To date, reports of solution structures determined through neutron diffraction are limited to species formed upon dissolution of simple salts.

Nuclear magnetic resonance (NMR) is also used to probe the hydration state of metal complexes in solution. If water exchange is slow enough, the metal-bound $H_2^{17}O$ resonance can be directly integrated to determine the number of water ligands (q). Most often, water exchange is too rapid and cannot be resolved from the bulk water signal.[25] For certain paramagnetic ions such as Dy(III) or Tb(III) that induce a large chemical shift without significant line broadening, the concentration-dependent change in the $H_2^{17}O$ resonance may be proportional to the hydration number.[26,27] Time-resolved luminescence can also be used to determine q, although this is limited to the lanthanides.

Unfortunately, none of these techniques are very useful for probing the hydration state of Mn(II). Moreover, one cannot

Chart 1. Mn(II) Complexes Explored in This Study

$[Mn(H_2O)_6]^{2+}$ $[Mn(9\text{-}ane\text{-}N_2O\text{-}2P)(H_2O)]^{2-}$ $[Mn_2(ENOTA)(H_2O)_2]$ $[Mn(15\text{-}pyN_3O_2)(H_2O)_2]^{2+}$ $[Mn(15\text{-}pyN_5)(H_2O)_2]^{2+}$

$[Mn(EDTA\text{-}BOM)(H_2O)]^{2-}$ $[Mn(EDTA\text{-}BOM_2)(H_2O)]^{2-}$ $[Mn(DTPA)]^{3-}$ $[Mn(CDTA)(H_2O)]^{2-}$ $[Mn(PMDPA)(H_2O)_2]$

$[Mn(LCyPh_2)(H_2O)]^{3-}$ $[Mn(HSA)(H_2O)_2]$
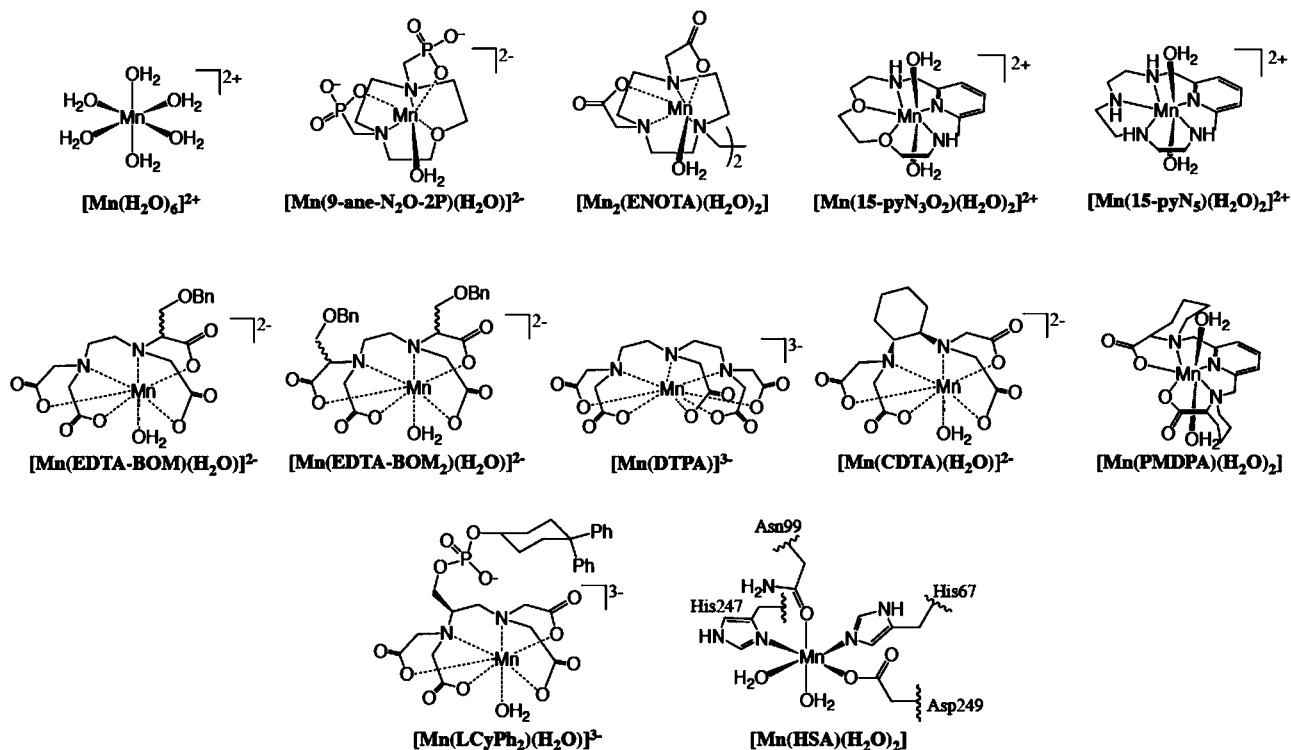
predict the hydration state by chemical intuition. The lack of ligand field stabilization energy results in no preference for specific coordination numbers or geometries. For instance, coordination numbers of five through eight have been observed crystallographically for high-spin Mn(II).[7,12,28−33] The coordination number of Mn(II) complexes varies even when held within ligand frameworks of identical denticity.

Determining the coordination number and hydration state of Mn(II) in solution is challenging. Yet understanding the hydration state of Mn(II) is critical in understanding the structure and function of Mn(II) species in chemistry and biology.

Mn(II) is biogenic, and trace Mn is a nutrient essential to the function of several enzymes and physiological processes.[34] For example, Mn plays a key role in antioxidant defense and serves as the transition metal cofactor utilized in catalase,[35,36] which disproportionates adventitious hydrogen peroxide, and as a metal cofactor in the superoxide dismutase isoform found in the eukaryotic mitochondria.[37−40] Mn(II) has also been shown to play a key structural role in certain DNA and RNA polymerases and kinases, among other enzymes performing essential life processes.[41−44] Mn homeostasis is a delicate balance, and Mn overload is associated with neurological decline characterized by symptoms similar to those associated with idiopathic Parkinson's disease, commonly referred to as manganism.[45] It is understood that Mn(II) accumulates in neurons through voltage-dependent Ca(II) channels and is subsequently shuttled around the nervous system. However, little information is known as to the speciation of Mn(II) in neurons, and the mechanisms of Mn(II) trafficking and homeostasis are largely unresolved and have been a subject of intense scrutiny.

High-spin Mn(II) ($S = 5/2$) is a potent T_1 relaxation agent that can be used to generate contrast in magnetic resonance imaging (MRI), and understanding hydration is key to understanding function.[46,47] For example, the neurological

activity of Mn(II) has been exploited for mapping neuronal structures and pathways, and this is done by administration of $MnCl_2$ to afford contrast in preclinical neuroimaging applications.[48−51] Mn(II) uptake has also been utilized as a measure of cell viability through correlating signal enhancement to cellular function. For example, this strategy has been used to track changes in β-cell mass in studies pertaining to the onset and progression of type I diabetes.[52] Mn(II) uptake in hepatocytes has also been used to visualize hepatic lesions.[53,54] However, the molecular forms of Mn(II) in the brain, pancreas, or liver are unknown. For example, does the Mn^{2+} aqua ion persist, or does it bind to an endogenous low molecular weight or macromolecular ligand? Probing Mn(II) hydration in these systems would begin to address such questions.

There is also a growing interest in developing stable Mn(II) coordination complexes for use as MRI relaxation agents.[12,31,32,55−62] The identification of nephrogenic systemic fibrosis, a rare but serious disorder associated with dissociated Gd(III),[63−65] coupled with a growing interest in MR probes capable of providing metabolic information to accompany structural images is the driving factor behind this growing body of research.[66−68] For example, our group is interested in exploiting the Mn(III/II) redox couple to design MR probes that are responsive to altered redox homeostasis associated with hypoxia or oxidative stress.[69]

Here we show that the peak transverse ^{17}O relaxivity, r^o_{2max}, of a Mn(II) complex reports directly on the hydration number. This result is predicated on the observation that the Mn(II)-induced increase in $H_2{}^{17}O$ line width is almost entirely due to water exchange at field strengths commonly utilized for NMR spectroscopy. We show that q can be determined for a range of Mn(II) complexes (Chart 1) and for Mn(II) associated with proteins.

■ RESULTS AND DISCUSSION

Relationship between Hydration Number and H$_2$^{17}O NMR Chemical Shift. High-spin Mn(II) complexes have no ligand field stabilization and are extremely labile. This results in very fast exchange of coordinated water ligand(s). The spin delocalization from the Mn(II) ion to the oxygen donor atom or proton on the water ligand is described by the hyperfine coupling constants $A_o/\hbar$ and $A_H/\hbar$, respectively. For Mn(II), one does not expect $A_o/\hbar$ to vary considerably regardless of the other ligand(s) in the complex. Literature values of $A_o/\hbar$ for Mn−^{17}OH$_2$ range from 2.6 to 4.1 × 10^7 rad/s, with the aqua ion having a hyperfine coupling constant in the middle of this range (3.3 × 10^7 rad/s).[57,73,74] There are fewer reports regarding $A_H/\hbar$, but hyperfine coupling constants between 3.8 and 6.3 × 10^6 rad/s have been reported for [Mn-(H$_2$O)$_6$]$^{2+}$.[75]

In principle, the paramagnetic shift of the ^{17}O or ^{1}H NMR signal induced by Mn(II) should yield the hydration number q. In the fast exchange regime (where the exchange rate k_{ex} is much larger than the transverse relaxation rate $(1/T_{2m})$ of the coordinated water; in Supporting Information), the paramagnetic chemical shift $\Delta\omega_p$ is given by eq 1, where ω_{ref} is the frequency of ^{17}O or ^{1}H in the absence of Mn(II), B_0 is the applied magnetic field, and the other symbols have their usual meanings.[75−77] Given the relative invariance in $A_o/\hbar$ (and presumably $A_H/\hbar$), Mn(II) should affect the chemical shift in a predictable manner. The hydration number should be readily attained from the slope of a plot of $\Delta\omega_p$ versus [Mn] at a fixed temperature. Alternately, one can estimate q from the dependence of $\Delta\omega_p$ on temperature.

$$\Delta\omega_p = \Delta\omega_{obs} - \Delta\omega_{ref} = \frac{q[Mn]}{[H_2O]}\frac{g_L S(S+1) B_0}{3k_B T}\left(\frac{A_o}{\hbar}\right) \quad (1)$$

In practice, this is very difficult because Mn(II) is such a potent relaxation agent and the inherent line widths are large, rendering accurate assignment of chemical shift difficult. This problem is explored in Figure 1 for [Mn(H$_2$O)$_6$]$^{2+}$, which displays calculated H$_2$^{17}O chemical shift and full width at half-height line width data (see below). Figure 1a shows the concentration-dependent chemical shift at 55 °C and 9.4 T in
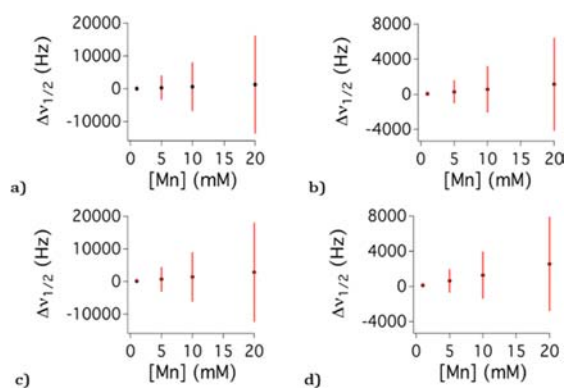
Figure 1. Concentration dependence on H$_2$^{17}O chemical shift (black dots) and line width at half-height (red bars) simulated from the previously reported hyperfine coupling constant, water exchange, and electronic relaxation parameters for [Mn(H$_2$O)$_6$]$^{2+}$ at various field strength and temperature: (a) 55 °C, 9.4 T; (b) 90 °C, 9.4 T; (c) 55 °C, 21 T; (d) 90 °C, 21 T.

hertz with line width at half-height ($\Delta\nu_{1/2}$) denoted as bars. For example, 10 mM Mn^{2+} changes the H$_2$^{17}O chemical shift by 640 Hz, but $\Delta\nu_{1/2}$ is 14 900 Hz. Increasing the temperature to 90 °C (Figure 1b) reduces the line width to 5300 Hz, but this is still much larger than the chemical shift (570 Hz), and the broad lines obscure precise assignment of chemical shift. Figure 1c,d shows the effect of moving to a higher field to increase the shift. Even at 21 T, the shifts are small relative to the line width. Calculated ^{1}H$_2$O chemical shift and half-height line width (Supporting Information Figure S1) depict similar difficulties.

Relationship between Hydration Number and Line Width. An alternate approach is to take advantage of the enhanced transverse relaxation rates. For Mn(II), the induced chemical shift is very small relative to the increase in signal line width. The observed paramagnetic relaxation rate $(1/T_{2p})$, and thus line width, is defined by the residency time of the water ligand (τ_m, the inverse of the water exchange rate, k_{ex}), T_{2m}, the Mn(II) concentration, and q (eq 2). When $T_{2m} \gg \tau_m$ (fast exchange regime), the observed paramagnetic relaxation rate will increase with decreasing temperature and reach a maximum where $T_{2m} = \tau_m$ and will then decrease as τ_m becomes larger than T_{2m}.

$$\frac{1}{T_{2p}} = \frac{1}{T_{2obs}} - \frac{1}{T_{2ref}} = \frac{q[Mn]}{[H_2O]}\frac{1}{T_{2m} + \tau_m} = \pi\Delta\nu_{1/2} \quad (2)$$

Relaxation of the coordinated H$_2$^{17}O is dominated by the scalar mechanism (eqs 3 and 4), which depends on the hyperfine coupling constant and a correlation time (τ_{sc}) that is dictated by either the water residency time or the T_{1e} of the unpaired electrons. Relaxation of the coordinated ^{1}H$_2$O occurs via multiple mechanisms and is discussed in the Supporting Information.

$$\frac{1}{T_{2m}} = \frac{S(S+1)}{3}\left(\frac{A_o}{\hbar}\right)^2 \tau_{sc} \quad (3)$$

$$\frac{1}{\tau_{sc}} = \frac{1}{T_{1e}} + \frac{1}{\tau_m} \quad (4)$$

For Mn(II), the electronic relaxation time increases with the square of the applied magnetic field.[78−80] Thus, at sufficiently high field, the correlation time for scalar relaxation (and T_{2m}) will be the water residency time τ_m. The implication of this condition is that at the maximum paramagnetic ^{17}O relaxation rate, where $T_{2m} = \tau_m$, one can rearrange eqs 2 and 3 and solve for q, eq 5.

$$q = r^o_{2max}[H_2O]\left(\frac{2}{\sqrt{\frac{S(S+1)}{3}}\frac{A_o}{\hbar}}\right) \cong \frac{r^o_{2max}}{510} \quad (5)$$

Here we introduce the term r^o_2 which is the transverse ^{17}O relaxivity, defined analogously to proton relaxivity ($\Delta(1/T_2)/$ [Mn]). In this case, we can calculate the maximum ^{17}O transverse relaxivity r^o_{2max} for a given q and hyperfine coupling constant. For the range of Mn−^{17}OH$_2$ hyperfine coupling constants, this leads to $r^o_{2max} = 510 \pm 100$ mM^{-1} s^{-1} per q. This is a powerful result because it means that q can be estimated from a few variable-temperature H$_2$^{17}O line width measurements. Using this method, we expect q can be solved within ±0.2 accuracy simply by fixing A_o/h to 3.3 × 10^7 rad/s. It should be noted that routinely employed chemical shift analysis

of Ln(III) complexes (excluding Gd(III)), which all exhibit short T_{1e} and thus narrow $\Delta\nu_{1/2}$, also yields q within ±0.2.[81]

To test the assumption that the water residency time dominates the scalar relaxation mechanism at high field ($\tau_m \ll T_{1e}$), we first examined the literature on Mn(II) complexes where electronic relaxation parameters were given (see Supporting Information and Table S1).[12,31,32,59,71,72,82] In this regard, we simulated the effects of varying temperature and applied field on r_2^o between 0 and 100 °C and 0.47 and 21 T. Figure 2 depicts the calculated dependence of r_{2max}^o on applied
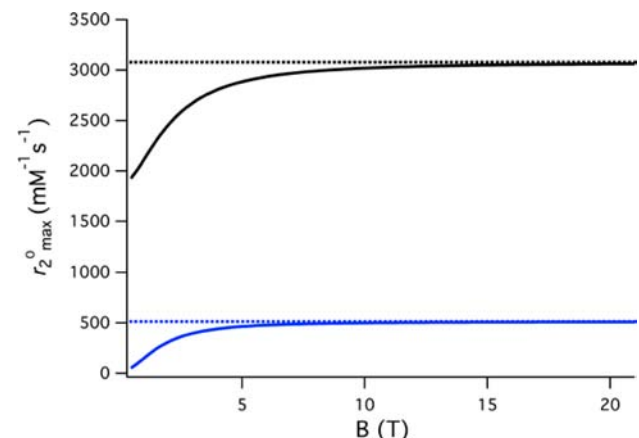
Figure 2. Simulated field dependence of r_{2max}^o for $[Mn(H_2O)_6]^{2+}$ (black) and $[Mn[9\text{-}ane\text{-}N_2O\text{-}2P)(H_2O)]^{2-}$ (blue). Dotted lines represent r_{2max}^o at ∞ T.

field for $[Mn(H_2O)_6]^{2+}$ and $[Mn(9\text{-}ane\text{-}N_2O\text{-}2P)(H_2O)]^{2-}$ (simulations for six other Mn(II) complexes are shown in Figures S1−S8) based on the reported hyperfine coupling constants, water exchange, and electronic relaxation parameters.[12,57,59,70,72] In Table 1, we list calculated r_{2max}^o values at 7,

Table 1. Simulated r_{2max}^o (mM^{-1} s^{-1}) Generated from the Hyperfine Coupling Constants, Water Exchange, and Electronic Relaxation Parameters of Previously Reported Mn(II) Complexes[12,32,59,70−72]

	7 T	11.7 T	21 T	∞ T
$[Mn(H_2O)_6]^{2+}$	2970	3037	3063	3076
$[Mn(9\text{-}ane\text{-}N_2O\text{-}2P)(H_2O)]^{2-}$	487	503	510	513
$[Mn_2(ENOTA)(H_2O)_2)]$	499	502	503	503
$[Mn(15\text{-}pyN_3O_2)(H_2O)_2]$	1121	1158	1178	1188
$[Mn(15\text{-}pyN_5)(H_2O)2]$	1171	1182	1186	1188
$[Mn(EDTA\text{-}BOM)(H_2O)]^{2-}$	564	576	581	584
$[Mn(EDTA\text{-}BOM_2)(H_2O)]^{2-}$	575	580	582	584
$[Mn(CDTA)(H_2O)]^{2-}$	371	393	402	406

11.7, 21, and ∞ T (where T_{1e} has no effect of scalar relaxation) for eight Mn(II) complexes from the literature. At 7 T, the effect of T_{1e} on r_{2max}^o is less than 9%, and this drops to 3% or less at 11.7 T. Thus, it would appear that the simple measurement of r_{2max}^o is a reasonable means to estimate q at field strengths used on modern NMR spectrometers.

To confirm these results, we measured the variable temperature r_2^o for four compounds with differing hydration state and water exchange kinetics. Figure 3 shows r_2^o as a function of temperature for $[Mn(H_2O)_6]^{2+}$, $[Mn(CDTA)(H_2O)]^{2-}$, $[Mn(PMPDA)(H_2O)_2]$, and $[Mn(DTPA)]^{3-}$. The relaxivities were measured at 9.4 and 11.7 T to assess the
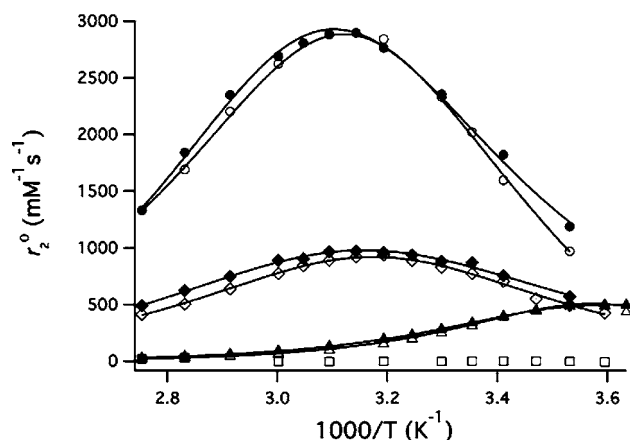
Figure 3. Plots of r_2^o as a function of temperature for $[Mn(H_2O)_6]^{2+}$ (circles), $[Mn(CDTA)(H_2O)]^{2-}$ (triangles), $[Mn(PMPDA)(H_2O)_2]$ (diamonds), and $[Mn(DTPA)]^{3-}$ (squares) at 9.4 T (solid symbols) and 11.7 T (open symbols). Solid lines represent fits to the data (see text).

influence of field on r_{2max}^o and are listed in Table 2. The hydration numbers estimated by this method are the same at 9.4 and 11.7 T and agree with the expected values based on crystal structures and analogous compounds.[70,72,83]

Table 2. Measured r_{2max}^o and Calculated Hydration Numbers (q) Using Equation 5 for $[Mn(H_2O)_6]^{2+}$, $[Mn(CDTA)(H_2O)]^{2-}$, and $[Mn(PMDPA)(H_2O)_2]$ at 9.4 and 11.7 T

	r_{2max}^o (mM^{-1} s^{-1})	q
$[Mn(H_2O)_6]^{2+}$ (9.4 T)	2970	5.79
$[Mn(H_2O)_6]^{2+}$ (11.7 T)	2840	5.54
$[Mn(CDTA)(H_2O)]^{2-}$ (9.4 T)	460	0.90
$[Mn(CDTA)(H_2O)]^{2-}$ (11.7 T)	460	0.90
$[Mn(PMDPA)(H_2O)_2]$ (9.4 T)	970	1.89
$[Mn(PMDPA)(H_2O)_2]$ (11.7 T)	940	1.83
$[Mn(DTPA)]^{3-}$ (11.7 T)	0	0

Water Exchange Kinetics. The data in Figure 3 can be analyzed to estimate water exchange kinetics for these three complexes. The rate constants and activation energies are listed in Tables 3−5 along with comparisons to previous studies. We analyzed the variable-temperature data in three ways, and χ^2 values are given to indicate the quality of the fits. In model 1, we fit the data to a four-parameter model by varying τ_m^{310}, T_{1e}^{310}, $\Delta H^\ddagger$, and ΔE_{T1e} (see Supporting Information) and assumed an exponential temperature dependence on water exchange and electronic relaxation.[84] Here we set q equal to the 1, 2, and 6 for $[Mn(CDTA)(H_2O)]^{2-}$, $[Mn(PMPDA)(H_2O)_2]$, and $[Mn(H_2O)_6]^{2+}$, respectively, and assumed a common hyperfine coupling constant of 3.3×10^7 rad/s. In this case, the data fit well but there were very large relative uncertainties associated with the electronic relaxation parameters, indicating that electronic relaxation does not contribute to the measured ^{17}O T_2 values. In model 2, we ignored the effect of electronic relaxation and fit the data to only two parameters: the water residency time at 310 K and the activation enthalpy for water exchange. As expected, the quality of the two-parameter fit is similar to the four-parameter fit in model 1. In model 3, we again ignored electronic relaxation but this time allowed the hyperfine coupling constant to vary. Model 3 gives equivalent

Table 3. Water Exchange and Electronic Relaxation Parameters Yielded by Three Different Fits of Temperature-Dependent Transverse H$_2$^{17}O Relaxation in the Presence of [Mn(H$_2$O)$_6$]$^{2+}$

	q	$A_o/\hbar$ (×10^7 rad/s)	τ_m^{310} (ns)	T_{1e} (ns)	$\Delta H^{\ddagger}$ (kJ/mol)	ΔE_{T1e} (kJ/mol)	χ^2
Lit. (ref 70)	6	3.33	27.3		32.9		
method 1 (9.4 T)	6	3.33	29.4 ± 0.9	471 ± 143	26.1 ± 1.1	−60.7. ± 7.5	0.0047
method 1 (11.7 T)	6	3.33	28.8 ± 10.8	321 ± 2410	32.0 ± 6.8	−17.4 ± 504	0.0085
method 2 (9.4 T)	6	3.33	26.5 ± 0.6		30.0 ± 0.6		0.0189
method 2 (11.7 T)	6	3.33	28.4 ± 0.5		32.7 ± 0.5		0.0124
method 3 (9.4 T)	6	3.18 ± 0.04	28.5 ± 0.5		28.5 ± 0.6		0.0073
method 3 (11.7 T)	6	3.23 ± 0.06	28.9 ± 0.6		31.7 ± 0.8		0.0091
average/std.			28.4 ± 1.3		30.0 ± 2.4	--	

Table 4. Water Exchange and Electronic Relaxation Parameters Yielded by Three Different Fits of Temperature-Dependent Transverse H$_2$^{17}O Relaxation in the Presence of [Mn(CDTA)(H$_2$O)]$^{2−}$

	q	$A_o/\hbar$ (×10^7 rad/s)	τ_m^{310} (ns)	T_{1e} (ns)	$\Delta H^{\ddagger}$ (kJ/mol)	ΔE_{T1e} (kJ/mol)	χ^2
Lit. (ref 72)	1	2.64	3.5		42.5		
method 1 (9.4 T)	1	3.33	4.4 ± 0.2	38 ± 10	28.0 ± 0.6	−33.3 ± 3.1	0.0018
method 1 (11.7 T)	1	3.33	3.7 ± 4.8	29 ± 375	35.9 ± 23.2	−37.3 ± 224	0.0341
method 2 (9.4 T)	1	3.33	3.9 ± 0		31.8 ± 0.4		0.0088
method 2 (11.7 T)	1	3.33	3.3 ± 0.1		35.6 ± 0.8		0.0475
method 3 (9.4 T)	1	3.25 ± 0.4	4.1 ± 0.1		31.9 ± 0.3		0.0067
method 3 (11.7 T)	1	3.14 ± 0.09	3.7 ± 0.2		35.8 ± 0.7		0.0344
average/std.			4.1 ± 0.6		33.2 ± 3.2		

Table 5. Water Exchange and Electronic Relaxation Parameters Yielded by Three Different Fits of Temperature-Dependent Transverse H$_2$^{17}O Relaxation in the Presence of [Mn(PMDPDA)(H$_2$O)$_2$]

	q	$A_o/\hbar$ (×10^7 rad/s)	τ_m^{310} (ns)	T_{1e} (ns)	$\Delta H^{\ddagger}$ (kJ/mol)	ΔE_{T1e} (kJ/mol)	χ^2
	2						
method 1 (9.4 T)	2	3.33	23.2 ± 0.7	292 ± 64	21.5 ± 1.2	−45.9 ± 7.8	0.0044
method 1 (11.7 T)	2	3.33	23.5 ± 1.5	100 ± 18	25.7 ± 1.6	−31.2 ± 12.6	0.0083
method 2 (9.4 T)	2	3.33	21.4 ± 0.5		24.8 ± 0.5		0.0170
method 2 (11.7 T)	2	3.33	21.0 ± 0.3		26.6 ± 0.3		0.0811
method 3 (9.4 T)	2	3.19 ± 0.03	22.0 ± 0.3		23.2 ± 0.5		0.0051
method 3 (11.7 T)	2	2.99 ± 0.03	23.2 ± 0.3		26.0 ± 0.4		0.0083
average/std.			23.2 ± 3.5		26.5 ± 3.6		

water exchange kinetic parameters but somewhat better fits. This is expected since the r_{2max}^o method gave slightly noninteger q values. By fixing q to integer values, the hyperfine constant will adjust to reflect this difference. The water exchange rate and enthalpy of activation are in good accord for all three models for the three complexes. The water exchange kinetic parameters were also consistent at both fields where measurements were made. These findings underscore the observation that electronic relaxation is sufficiently long and negligibly affects T_{2m} at these field strengths.

Sensitivity and Scope of q Determination. Because Mn(II) is such a potent relaxation agent, this method of q estimation can be used at submillimolar concentrations. The main limitation is the fast diamagnetic relaxation of H$_2$^{17}O which increases with decreasing temperature. If we conservatively assume that, at peak relaxivity, the paramagnetic relaxation rate should contribute 10% of the observed relaxation rate, then one would only require between 10 and 50 μM Mn(II) for a q = 1 complex, depending on the temperature of r_{2max}^o (higher sensitivity at higher temperatures). Because crossover into the fast exchange regime must occur between 0 and 100 °C to identify r_{2max}^o, this method cannot be successfully applied to complexes that display extremely fast exchange kinetics (τ_m^{310} < 2 ns), in which case T_{2m} = τ_m occurs below the freezing point of water, or complexes that display

very slow exchange kinetics (τ_m^{310} > 200 ns). However, water exchange rates of all Mn(II) complexes reported to date, including the compounds in this study, fall within this range, suggesting that this methodology should be ideally suited for the study of most Mn(II) complexes.

Extension to Complex:Protein Interactions. The relatively high sensitivity of this technique allows for the interrogation of hydration number for Mn(II) complexes interacting with proteins. As an example, we investigated [Mn[EDTACyPh$_2$)(H$_2$O)]$^{3−}$ as a function of temperature in 4.5% w/v human serum albumin (HSA) at pH 7.4 (50 mM HEPES buffer). In this case, $1/T_{2ref}$ was determined from the temperature dependence of a HSA solution that contained no Mn(II). [Mn[EDTACyPh$_2$)(H$_2$O)]$^{3−}$ was designed to noncovalently bind to drug binding site 2 of HSA, a hydrophobic pocket associated with the binding and transport of lipophilic substrates. This complex has been shown to be 98% protein-bound at 310 K at the concentration employed in this experiment (0.1 mM).[85] ^{1}H relaxometry methods performed on [Mn[EDTACyPh$_2$)(H$_2$O)]$^{3−}$ in HSA suggest contributions from a Mn(II)-coordinated water to T_1 relaxation, but the hydration state of the Mn(II) ion in this adduct has not been formally probed.

The temperature-dependent r_{2max}^o of [Mn(EDTACyPh$_2$)-(H$_2$O)]$^{3−}$ recorded in neat H$_2$O and HSA solution is shown in

Figure 4; the hydration state estimated from r^o_{2max}, and relevant exchange parameters are tabulated in Table 6. The calculated
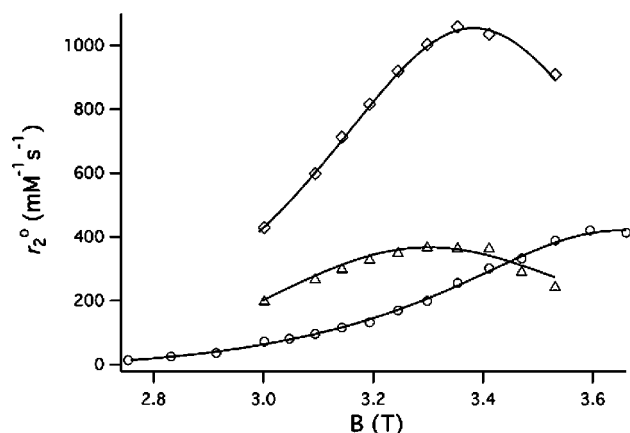
Figure 4. Transverse ^{17}O relaxivity, r^o_2, as a function of temperature at 11.7 T for $[Mn[EDTACyPh_2)(H_2O)]^{3-}$ in water (circles) and in 4.5% w/v HSA at pH 7.4 (triangles), and the Mn(II)−HSA complex at pH 8.6 (diamonds). Solid lines represent fits to the data (see text).

hydration state of 0.72 of HSA-bound $[Mn(EDTACyPh_2)-(H_2O)]^{3-}$ suggests the possibility of some $q = 0$ species present. It is known that protein side chains can displace water ligands in Gd(III) complexes when bound to HSA,[5,86] although this is typically seen with $q = 2$ complexes. The water exchange rate of $[Mn(EDTACyPh_2)(H_2O)]^{3-}$ is 4-fold slower when the complex is bound to HSA and highlights the fact that HSA binding strongly influences the interaction of this complex with bulk water. This study highlights the sensitivity of Mn(II)-induced relaxation to probe hydration and water exchange kinetics for protein-bound complexes.

Extension to Metalloproteins. As a second example, we sought to determine the hydration number of the Mn(II) ion when it was coordinated by human serum albumin (HSA). In the presence of HSA, Mn(II) binds preferentially to a motif denoted multimetal binding site A, found at the interface of two subdomains (I and II) and comprising His67, Asn99, His247, and Asp249.[87] This mixed N/O binding site is conserved throughout all mammalian serum albumins. The affinity for multimetal site A for Mn(II) has been studied as a function of pH, Mn(II) concentration, and concentration of competitor ions and substrates through proton relaxation enhancement techniques.[87−89] As a result, the interaction of Mn(II) and HSA is relatively well-defined. However, the solution structure of the Mn(II) ion in multimetal site A has never been explored.

The r^o_2 of Mn(II)−HSA as a function of temperature was recorded at 0.1 mM and pH 8.6 (50 mM Tris buffer) (Figure 4). Under these conditions, we can expect Mn(II) to exclusively reside in site A.[87] A hydration state of $q = 2$ was calculated from the r^o_{2max} value; the water exchange parameters are listed in

Table 6. Previous study of Zn(II) housed within site A by EXAFS suggests five-coordinate Zn(II), bound by the aforementioned residues and one water.[90] The backbone carbonyl of His247 was also found to interact with the Zn(II) ion, but the Zn−O distance is too large for this donor to be considered a part of the primary coordination sphere. The bis(aquated) nature of the Mn(II) adduct is likely a result of the expanded radius of the Mn(II) ion relative to Zn(II). We note that we could successfully reproduce this result using a solution containing 25 μM Mn(II), which further highlights the sensitivity of this method for biomolecule applications.

Comparison of Mn(II) Water Exchange Kinetics. The τ_m^{310} values recorded for $[Mn(H_2O)_6]^{2+}$, $[Mn(CDTA)-(H_2O)]^{2-}$, and $[Mn(EDTACyPh_2)(H_2O)]^{3-}$ agree with those obtained previously. This study is the first report on the exchange kinetics measured by ^{17}O transverse relaxation rates for the $q = 2$ complex $[Mn(PMDPA)(H_2O)_2]$. The exchange kinetics of $[Mn(PMDPA)(H_2O)_2]$ fall within the range defined by the handful of Mn(II) complexes housed within rigid, pentadentate ligands.[32,82,91] We found that $[Mn-(EDTACyPh_2)(H_2O)]^{3-}$ underwent 4-fold slower water exchange upon protein binding. A decrease in water exchange rate has also been observed for Gd(III) complexes binding to HSA.[92−94] Hydrogen bonding to the coordinated water molecule by protein side chains in the binding pocket may slow water exchange. Mn^{2+} bound to HSA has been previously studied at pH 7.0 by ^1H NMRD and ^{17}O NMR at 2.1 T, and a τ_m^{310} of 12−15 ns was reported. However, histidine (pK_a ~6.7) coordination to Mn(II) at multimetal binding site A is pH-dependent, and it is likely that the Mn(II) species explored in that study is different than that recorded here.

Extension of Technique to Gd(III) Complexes. Given the similarity in relaxation mechanisms between Mn(II) and Gd(III), and because of the importance of hydration state in the application of Gd(III) complexes as MRI contrast agents, we investigated whether the r^o_{2max} approach could be taken with Gd(III). The hyperfine coupling constant $A_o/\hbar$ for Gd−$^{17}OH_2$ is well-established from NMR and EPR studies to be 3.8×10^6 rad/s,[95] and this leads to $r^o_{2max} = 78$ mM^{-1} s^{-1} per q in the absence of contributions from T_{1e}.

We retrospectively analyzed some data obtained at 7 T for eight different Gd(III) complexes based on DOTA or DTPA ligands (Figure S10 and Table S2) and of known hydration state.[96]

These compounds showed a range of r^o_{2max} values from 22 to 33 mM^{-1} s^{-1} per q. These r^o_{2max} values are far from the value predicted if there is no contribution to scalar relaxation from T_{1e}. Indeed, the T_{1e} values for these complexes are comparable to τ_m, and the assumptions leading to eq 5 break down.

We also made some relaxation rate measurements at 11.7 T on $[Gd(DTPA)(H_2O)]^{2-}$, $[Gd(HPDO3A)(H_2O)]$, $[Gd-(DTPA-BMA)(H_2O)]$, $[Gd(DOTAla)(H_2O)]$,[97] and $[Gd-(CyPic3A)(H_2O)_2]^{-98}$ (Figure S11 and Table S3). The $r^o_{2max}/$

Table 6. Water Exchange Parameters Obtained Using Model 1 ($A_o/\hbar = 3.3 \times 10^7$ rad/s) from the Temperature-Dependent Transverse Relaxation in the Presence of $[Mn(EDTACyPh_2)(H_2O)]^{3-}$ in Water and in 4.5% w/v HSA, and for Mn(II) Ligated by Multimetal Binding Site A of HSA; q (Fit) Denotes the q Value Used in the Fitting Procedure

	r^o_{2max} (mM^{-1} s^{-1})	q (calcd)	q (fit)	τ_m^{310} (ns)	T_{1e} (ns)	$\Delta H^{\ddagger}$ (kJ/mol)	$\Delta E_{T_{1e}}$ (kJ/mol)	χ^2
$[Mn(EDTACyPh_2)(H_2O)]^{3-}$	430	0.84	1	3.3 ± 0.5	21 ± 18	21.1 ± 3.8	−73.4 ± 13.1	0.0594
$[Mn(EDTACyPh_2)(H_2O)]^{3-}$·HSA	340	0.66	0.7	13.7 ± 2.3	803 ± 2600	26.4 ± 5.7	−11.6 ± 61.0	0.0461
Mn(II)·HSA	1060	2.06	2	9.4 ± 0.3	1239 ± 4290	30.6 ± 1.1	−77.4 ± 44.3	0.0012

q values at this field strength ranged between 25.2 and 40.9 mM^{-1} s^{-1}. It is apparent that the r^o_{2max} values measured at 11.7 T are still far from approaching the ∞ T limit (where T_{1e} is negligible). Thus, variations in T_{1e} induced by either changes in magnetic field or differences in the ligand field make q determination by this technique unpredictable. For example, r^o_{2max}/q for [Gd(DOTAla)(H$_2$O)] is 62% greater than the value measured for [Gd(HPDO3A)(H$_2$O)].

Figure 5 shows the dependence of r^o_{2max} on external field for [Gd(HPDO3A)(H$_2$O)] simulated from recently reported zero-
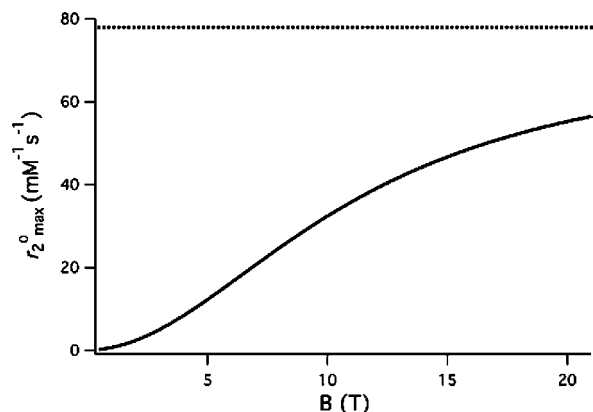
Figure 5. Simulated field dependence of r^o_2 for [Gd(HPDO3A)(H$_2$O)] at 49 °C; r^o_{2max} occurs at this temperature at 5 T and above. Dotted line represents r^o_{2max} at ∞ T.

field splitting parameters.[99] This plot is generally reflective of all Gd(III) complexes considered in this study. Although direct measurement of r^o_{2max} may not represent a reliable method to estimate q for Gd(III), there exist numerous reliable strategies to obtain this value.[26,27,81,100]

The failure of this method applied to Gd(III) is best understood in terms of the nature of the interaction between the coordinated water and unpaired electrons. As a result of lanthanide contraction, the 4f electrons of Gd(III) are well-shielded and interact weakly with the coordinated H$_2$^{17}O, whereas the 3d electrons of Mn(II) are much more accessible. The mechanism of spin delocalization from Gd(III) to H$_2$^{17}O is inefficient relative to Mn(II), which results in nearly an order of magnitude difference in hyperfine coupling constant. In turn, the relaxation time for a coordinated water ligand (T_{2m}) to Mn(II) is nearly an order of magnitude shorter than for a water coordinated to Gd(III) with equivalent water exchange kinetics and electronic relaxation. Because r^o_{2max} is achieved when $T_{2m} = \tau_m$, the mean water residency time at this event will be significantly shorter for a Mn(II) complex than for a Gd(III) complex with similar electronic relaxation. For instance, although the r^o_{2max} of [Mn(H$_2$O)$_6$]$^{2+}$ and [Gd(HPDO3A)-(H$_2$O)] occurs at similar temperatures (45−50 °C), their water residency times at this maximum are 18 and 113 ns, respectively. Because τ_m at r^o_{2max} is much shorter for Mn(II), the influence of T_{1e} on T_{2m} is negligible at high fields and the approximations leading to eq 5 are valid.

CONCLUSION

The hydration state of Mn(II) can be inferred directly from H$_2$^{17}O line widths. This is because longitudinal electronic relaxation affects Mn(II)-induced T_2 relaxation only negligibly at magnetic fields found on modern NMR spectrometers. This

phenomenon was validated through simulations of r^o_2 as a function of temperature and field strength corresponding to eight Mn(II) complexes from the literature for which electronic relaxation parameters are reported and through measurement of seven unique Mn(II) complexes at 9.4 and/or 11.7 T. Due to the tremendous line-broadening effect of Mn(II), this information can be obtained using micromolar Mn(II) concentrations. In this regard, this technique was successfully extended to measure the hydration state and water exchange parameters of a Mn(II) complex noncovalently bound to HSA and to Mn(II) directly coordinated by HSA. We anticipate that this simple NMR technique will find great utility in future studies directed toward understanding the solution structure of Mn(II)-containing species.

■ EXPERIMENTAL SECTION

General. All materials were purchased commercially, except for PMDPA, which was prepared as reported.[83] NMR spectra were recorded on either a 9.4 or 11.7 T Varian spectrometer equipped with a 5 mm broad-band probe. The transverse relaxation times of ^{17}O were measured through the line width of the H$_2$^{17}O NMR signal at half-height.[92] The values obtained through this method were in excellent agreement with those obtained using the CPMG pulse sequence. Relaxivity was calculated by dividing the Mn(II) or Gd(III) imparted increase in $1/T_2$ relative to neat H$_2$O at pH 3 by the concentration of the paramagnetic ion in mM. For samples in HSA solution, the increase in relaxation rate was measured relative to the HSA solution alone at the same temperature. Samples were enriched to contain between 0.1 and 0.2% H$_2$^{17}O. Samples were prepared by adding slightly substoichiometric quantities of Mn(II) or Gd(III) to the ligand solution to ensure full ion chelation, and the pH was adjusted to ~6.5 for complexes of Gd(III) or to pH 7−8 for complexes of Mn(II). [Mn(PMDPA)(H$_2$O)$_2$] was prepared by adding Mn(II) to ligand in 50 mM HEPES buffer at pH 7.4. The pH was measured using a ThermoOrion pH meter connected to a VWR Symphony glass electrode. Mn and Gd concentrations were determined using an Agilent 7500a ICP-MS system. All samples were diluted with 0.1% Triton X-100 in 5% nitric acid containing 20 ppb of Lu (as internal standard). The ratio of Mn (54.94) or Gd (157.25)/Lu (174.97) was used to quantify the metal concentration. A linear calibration curve ranging from 0.1 to 200 ppb was generated daily for the quantification.

■ ASSOCIATED CONTENT

S Supporting Information
Descriptions of the equations that define relaxation and two-site exchange, additional simulations and tables describing hyperfine coupling constant, water exchange, and transient ZFS parameters of previously reported Mn(II) and Gd(III) complexes and a table describing water exchange and electronic relaxation of Gd(III) complexes at 7 and 11.7 T. This material is available free of charge via the Internet at http://pubs.acs.org.

■ AUTHOR INFORMATION

Corresponding Author
caravan@nmr.mgh.harvard.edu

Present Address
†Sichuan Key Laboratory of Medical Imaging, North Sichuan Medical College, Nanchong City, Sichuan, 637007, China.

Notes
The authors declare no competing financial interest.

■ REFERENCES

(1) Bostick, D. L.; Brooks, C. L., III. *Proc. Natl. Acad. Sci. U.S.A.* **2007**, *104*, 9260.

(2) Yu, H.; Noskov, S. Y.; Roux, B. *J. Phys. Chem. B* **2009**, *113*, 8725.

(3) Bernasconi, L.; Baerends, E. J. *J. Am. Chem. Soc.* **2013**, *135*, 8857.

(4) Lowe, M. P.; Parker, D.; Reany, O.; Aime, S.; Botta, M.; Castellano, G.; Gianolio, E.; Pagliarin, R. *J. Am. Chem. Soc.* **2001**, *123*, 7601.

(5) Moriggi, L.; Yaseen, M. A.; Helm, L.; Caravan, P. *Chem.—Eur. J.* **2012**, *18*, 3675.

(6) Garcia-Martin, M. L.; Martinez, G. V.; Raghunand, N.; Sherry, A. D.; Zhang, S.; Gillies, R. J. *Magn. Reson. Med.* **2006**, *55*, 309.

(7) Dube, K. S.; Harrop, T. C. *Dalton Trans.* **2011**, *40*, 7496.

(8) Diebold, A.; Hagen, K. S. *Inorg. Chem.* **1998**, *37*, 215.

(9) Gale, E. M.; Cowart, D. M.; Scott, R. A.; Harrop, T. C. *Inorg. Chem.* **2011**, *50*, 10460.

(10) Leitch, S.; Bradley, M. J.; Rowe, J. L.; Chivers, P. T.; Maroney, M. J. *J. Am. Chem. Soc.* **2007**, *129*, 5085.

(11) Herbst, R. W.; Perovic, I.; Martin-Diaconescu, V.; O'Brien, K.; Chivers, P. T.; Pochapsky, S. S.; Pochapsky, T. C.; Maroney, M. J. *J. Am. Chem. Soc.* **2010**, *132*, 10338.

(12) Drahoš, B.; Pniok, M.; Havlíčková, J.; Kotek, J.; Císařová, I.; Hermann, P.; Lukeš, I.; Tóth, E. *Dalton Trans.* **2011**, *40*, 10131.

(13) Gezahegne, W. A.; Hennig, C.; Tsushima, S.; Planer-Friedrich, B.; Scheinost, A. C.; Merkel, B. J. *Environ. Sci. Technol.* **2012**, *46*, 2228.

(14) Moll, H.; Denecke, M. A.; Jalilehvand, F.; Sandström, M.; Grenthe, I. *Inorg. Chem.* **1999**, *38*, 1795.

(15) Spångberg, D.; Hermansson, K.; Lindqvist-Reis, P.; Jalilehvand, F.; Sandström, M.; Persson, I. *J. Phys. Chem. B* **2000**, *104*, 10467.

(16) Frank, P.; Benfatto, M.; Hedman, B.; Hodgson, K. O. *Inorg. Chem.* **2012**, *51*, 2086.

(17) Migliorati, V.; Mancini, G.; Tatoli, S.; Zitolo, A.; Filipponi, A.; De Panfilis, S.; Di Cicco, A.; D'Angelo, P. *Inorg. Chem.* **2013**, *52*, 1141.

(18) Atta-Fynn, R.; Bylaska, E. J.; de Jong, W. A. *J. Phys. Chem. Lett.* **2013**, *4*, 2166.

(19) Bowron, D. T.; Beret, E. C.; Martin-Zamora, E.; Soper, A. K.; Marcos, E. S. *J. Am. Chem. Soc.* **2012**, *134*, 962.

(20) Jalilehvand, F.; Spångberg, D.; Lindqvist-Reis, P.; Hermansson, K.; Persson, I.; Sandström, M. *J. Am. Chem. Soc.* **2001**, *123*, 431.

(21) Varma, S.; Rempe, S. B. *Biophys. Chem.* **2006**, *124*, 192.

(22) Ansell, S.; Barnes, A. C.; Mason, P. E.; Neilson, G. W.; Ramos, S. *Biophys. Chem.* **2006**, *124*, 171.

(23) Hewish, N. A.; Neilson, G. W.; Enderby, J. E. *Nature* **1982**, *297*, 138.

(24) Mile, V.; Gereben, O.; Kohara, S.; Pusztai, L. *J. Phys. Chem. B* **2012**, *116*, 9758.

(25) Helm, L.; Merbach, A. E. *Chem. Rev.* **2005**, *105*, 1923.

(26) Alpoin, M. C.; Urbano, A. M.; Geraldes, C. F. G. C.; Peters, J. A. *J. Chem. Soc., Dalton Trans.* **1992**, 463.

(27) Djanashvili, K.; Peters, J. A. *Contrast Media Mol. Imaging* **2007**, *2*, 67.

(28) Erre, L. S.; Micera, G.; Garribba, E.; Bényei, A. C. *New J. Chem.* **2000**, *24*, 725.

(29) Xiang, D. F.; Duan, C. Y.; Tan, X. S.; Hang, Q. W.; Tang, W. X. *J. Chem. Soc., Dalton Trans.* **1998**, 1201.

(30) Polyakova, I. N.; Sergienko, V. S.; Poznyak, A. L. *Crystallog. Rep.* **2002**, *47*, 280.

(31) Drahoš, B.; Kotek, J.; Císařová, I.; Hermann, P.; Helm, L.; Lukeš, I.; Tóth, E. *Inorg. Chem.* **2011**, *50*, 12785.

(32) Drahoš, B.; Kotek, J.; Hermann, P.; Lukeš, I.; Tóth, E. *Inorg. Chem.* **2010**, *49*, 3224.

(33) Wang, S.; Westmoreland, T. D. *Inorg. Chem.* **2009**, *48*, 719.

(34) Reddi, A. R.; Jensen, L. T.; Culotta, V. C. *Chem. Rev.* **2009**, *109*, 4722.

(35) Waldo, G. S.; Yu, S.; Penner-Hahn, J. E. *J. Am. Chem. Soc.* **1992**, *114*, 5869.

(36) Ivancich, A.; Barynin, V. V.; Zimmermann, J.-L. *Biochemistry* **1995**, *34*, 6628.

(37) Borgstahl, G. E. O.; Parge, H. E.; Hickey, M. J.; Beyer, W. F.; Hallewell, R. A.; Tainer, J. A. *Cell* **1992**, *71*, 107.

(38) Guan, Y.; Hickey, M. J.; Borgstahl, G. E. O.; Hallewell, R. A.; Lepock, J. R.; O'Connor, D.; Hsieh, Y. S.; Nick, H. S.; Silverman, D. N.; Tainer, J. A. *Biochemistry* **1998**, *37*, 4722.

(39) Hsieh, Y. S.; Guan, Y.; Tu, C. K.; Bratt, P. J.; Angerhofer, A.; Lepock, J. R.; Hickey, M. J.; Tainer, J. A.; Nick, H. S.; Silverman, D. N. *Biochemistry* **1998**, *37*, 4731.

(40) Hearn, A. S.; Fan, L.; Lepock, J. R.; Luba, J. P.; Greenleaf, W. B.; Cabelli, D. E.; Tainer, J. A.; Nick, H. S.; Silverman, D. N. *J. Biol. Chem.* **2004**, *279*, 5861.

(41) Lovitt, B.; VanderPorten, E. C.; Sheng, Z.; Zhu, H.; Drummond, J.; Liu, Y. *Biochemistry* **2010**, *49*, 3092.

(42) Unciuleac, M.-C.; Shuman, S. *Biochemistry* **2013**, *52*, 2967.

(43) Blanca, G.; Shevelev, I.; Ramadan, K.; Villani, G.; Spadari, S.; Hübscher, U.; Maga, G. *Biochemistry* **2003**, *42*, 7467.

(44) Zakharova, E.; Wang, J.; Konigsberg, W. *Biochemistry* **2004**, *43*, 6587.

(45) Benedetto, A.; Au, C.; Aschner, M. *Chem. Rev.* **2009**, *109*, 4862.

(46) Lauffer, R. B. *Chem. Rev.* **1987**, *87*, 901.

(47) Caravan, P.; Farrar, C. T.; Frullano, L.; Uppal, R. *Contrast Media Mol. Imaging* **2009**, *4*, 89.

(48) Daoust, A.; Barbier, E. L.; Bohic, S. *NeuroImage* **2013**, *64*, 10.

(49) Lindsey, J. D.; Grob, S. R.; Scadeng, M.; Duong-Polk, K.; Weinreb, R. N. *Magn. Reson. Imaging* **2013**, *31*, 865.

(50) Jin, S.-U.; Lee, J.-J.; Hong, K. S.; Han, M.; Park, J.-W.; Lee, H. J.; Lee, S.; Lee, K.-y.; Shim, K. M.; Cho, J. H.; Cheong, C.; Chang, Y. *Magn. Reson. Imaging* **2013**, *31*, 1143.

(51) Jelescu, I. O.; Nargeot, R.; Le Bihan, D.; Ciobanu, L. *NeuroImage* **2013**, *76*, 264.

(52) Dhyani, A. H.; Fan, X.; Leoni, L.; Haque, M.; Roman, B. B. *Magn. Reson. Imaging* **2013**, *31*, 508.

(53) Chung, J.-J.; Kim, M.-J.; Kim, K. W. *J. Magn. Res. Imaging* **2006**, *23*, 706.

(54) Elizondo, G.; Fretz, C. J.; Stark, D. D.; Rocklage, S. M.; Quay, S. C.; Worah, D.; Tsang, Y. M.; Chen, M. C.; Ferrucci, J. T. *Radiology* **1991**, *178*, 73.

(55) Pan, D.; Schmeider, A. H.; Wickline, S. A.; Lanza, G. M. *Tetrahedron* **2011**, *67*, 8431.

(56) Drahoš, B.; Kubíček, V.; Bonnet, C. S.; Hermann, P.; Lukeš, I.; Tóth, E. *Dalton Trans.* **2011**, *40*, 1945.

(57) Drahoš, B.; Lukeš, I.; Tóth, E. *Eur. J. Inorg. Chem.* **2012**, 1974.

(58) Rocklage, S. M.; Cacheris, W. P.; Quay, S. C.; Hahn, F. E.; Raymond, K. N. *Inorg. Chem.* **1989**, *28*, 477.

(59) Aime, S.; Anelli, P. L.; Botta, M.; Brocchetta, M.; Canton, S.; Fedeli, F.; Gianolio, E.; Terreno, E. *J. Biol. Inorg. Chem.* **2002**, *7*, 58.

(60) Zhang, Q.; Gorden, J. D.; Beyers, R. J.; Goldsmith, C. R. *Inorg. Chem.* **2011**, *50*, 9365.

(61) Kálmán, F. K.; Tircsó, G. *Inorg. Chem.* **2012**, *51*, 10065.

(62) Tei, L.; Gugliotta, G.; Fekete, M.; Kálmán, F. K.; Botta, M. *Dalton Trans.* **2011**, *40*, 2025.

(63) Di Gregorio, E.; Gianolio, E.; Stefania, R.; Barutello, G.; Digilio, G.; Aime, S. *Anal. Chem.* **2013**, *85*, 5627.

(64) Martin, D. R. *Am. J. Kidney Dis.* **2010**, *56*, 427.

(65) Stratta, P.; Canavese, C.; Quaglia, M.; Fenoglio, R. *Rheumatology* **2010**, *49*, 821.

(66) De Leon-Rodriguez, L. M.; Lubag, A. J. M.; Malloy, C. R.; Martinez, G. V.; Gillies, R. J.; Sherry, A. D. *Acc. Chem. Res.* **2009**, *42*, 948.

(67) Aime, S.; Botta, M.; Gianolio, E.; Terreno, E. *Angew. Chem., Int. Ed.* **2000**, *39*, 747.

(68) Yu, M.; Beyers, R. J.; Gorden, J. D.; Cross, J. N.; Goldsmith, C. R. *Inorg. Chem.* **2012**, *51*, 9153.

(69) Loving, G. S.; Mukherjee, S.; Caravan, P. *J. Am. Chem. Soc.* **2013**, *135*, 4623.

(70) Ducommun, Y.; Newman, K. E.; Merbach, A. E. *Inorg. Chem.* **1980**, *19*, 3696.

(71) Balogh, E.; He, Z.; Hsieh, W.; Liu, S.; Tóth, E. *Inorg. Chem.* **2007**, *46*, 238.

(72) Maigut, J.; Meier, R.; Zahl, A.; van Eldik, R. *Inorg. Chem.* **2008**, *47*, 5702.

(73) Zetter, M. S.; Grant, M. W.; Wood, E. J.; Dodgen, H. W.; Hunt, J. P. *Inorg. Chem.* **1972**, *11*, 2701.

(74) Rolla, G. A.; Platas-Iglesias, C.; Botta, M.; Tei, L.; Helm, L. *Inorg. Chem.* **2013**, *52*, 3268.

(75) Bertini, I.; Luchinat, C. NMR of Paramagnetic Substances. In *Coordination Chemistry Reviews*; Lever, A. B. P., Ed.; Elsevier: Amsterdam, 1996; Vol. 150. pp 43, 77−110.

(76) Bertini, I.; Fernández, C. O.; Karlsson, B. G.; Leckner, J.; Luchinat, C.; Malmström, B. G.; Nersissian, A. M.; Pierattelli, R.; Shipp, E.; Valentine, J. S.; Vila, A. J. *J. Am. Chem. Soc.* **2000**, *122*, 3701.

(77) Bertini, I.; Turano, P.; Villa, A. J. *Chem. Rev.* **1993**, *93*, 2833.

(78) Bloembergen, N.; Morgan, L. O. *J. Chem. Phys.* **1961**, *34*, 842.

(79) Sur, S. K.; Bryant, R. G. *J. Phys. Chem.* **1995**, *99*, 6301.

(80) Miller, J. C.; Sharp, R. R. *J. Phys. Chem. A* **2000**, *104*, 4889.

(81) Manus, L. M.; Strauch, R. C.; Hung, A. H.; Eckermann, A. L.; Meade, T. J. *Anal. Chem.* **2012**, *84*, 6278.

(82) Lieb, D.; Friedel, F. C.; Yawer, M.; Zahl, A.; Khusniyarov, M. M.; Heinemann, F. W.; Ivanović-Burmazović, I. *Inorg. Chem.* **2013**, *52*, 222.

(83) Su, H.; Wu, C.; Zhu, J.; Miao, T.; Wang, D.; Xia, C.; Zhao, X.; Gong, Q.; Song, B.; Ai, H. *Dalton Trans.* **2012**, *41*, 14480.

(84) Caravan, P.; Parigi, G.; Chasse, J. M.; Cloutier, N. J.; Ellison, J. J.; Lauffer, R. B.; Luchinat, C.; McDermid, S. A.; Spiller, M.; McMurry, T. J. *Inorg. Chem.* **2007**, *46*, 6632.

(85) Troughton, J. S.; Greenfield, M. T.; Greenwood, J. M.; Dumas, S.; Wiethoff, A. J.; Wang, J.; Spiller, M.; McMurry, T. J.; Caravan, P. *Inorg. Chem.* **2004**, *43*, 6313.

(86) Zech, S. G.; Sun, W.-C.; Jacques, V.; Caravan, P.; Astashkin, A. V.; Raitsimring, A. M. *ChemPhysChem* **2005**, *6*, 2570.

(87) Fanali, G.; Cao, Y.; Ascenzi, P.; Fasano, M. *J. Inorg. Biochem.* **2012**, *117*, 198.

(88) Aime, S.; Canton, C.; Crich, S. G.; Terreno, E. *Magn. Reson. Chem.* **2002**, *40*, 41.

(89) Mildvan, A. S.; Cohn, M. *Biochemistry* **1963**, *2*, 910.

(90) Blindauer, C. A.; Harvey, I.; Bunyan, K. E.; Stewart, A. J.; Sleep, D.; Harrison, D. J.; Berezenko, S.; Sadler, P. J. *J. Biol. Chem.* **2009**, *284*, 23116.

(91) Dees, A.; Zahl, A.; Puchta, R.; van Eikama Hommes, N. J. R.; Heinemann, F. W.; Ivanović-Burmazović, I. *Inorg. Chem.* **2007**, *46*, 2459.

(92) Zech, S. G.; Eldredge, H. B.; Lowe, M. P.; Caravan, P. *Inorg. Chem.* **2007**, *46*, 3576.

(93) Caravan, P.; Cluotier, N. J.; Greenfield, M. T.; McDermid, S. A.; Dunham, S. U.; Bulte, J. W. M.; Amedio, J. C., Jr.; Looby, R. J.; Supkowski, R. M.; Horrocks, W. D., Jr.; McMurry, T. J.; Lauffer, R. B. *J. Am. Chem. Soc.* **2002**, *124*, 3152.

(94) Eldredge, H. B.; Spiller, M.; Chasse, J. M.; Greenwood, M. T.; Caravan, P. *Invest. Radiol.* **2006**, *41*, 229.

(95) Caravan, P.; Astashkin, A. V.; Raitsimring, A. M. *Inorg. Chem.* **2003**, *42*, 3972.

(96) Dumas, S.; Jacques, V.; Sun, W.-C.; Troughton, J. S.; Welch, J. T.; Chasse, J. M.; Schmitt-Willich, H.; Caravan, P. *Invest. Radiol.* **2010**, *45*, 600.

(97) Boros, E.; Polasek, M.; Zhang, Z.; Caravan, P. *J. Am. Chem. Soc.* **2012**, *134*, 19858.

(98) Gale, E. M.; Kenton, N.; Caravan, P. *Chem. Commun.* **2013**, *49*, 8060.

(99) Castelli, D. D.; Caligara, M. C.; Bota, M.; Terreno, E.; Aime, S. *Inorg. Chem.* **2013**, *52*, 7130.

(100) Beeby, A.; Clarkson, I. M.; Dickins, R. S.; Faulkner, S.; Parker, D.; Royle, L.; de Sousa, A. S.; Williams, J. A. G.; Woods, M. *J. Chem. Soc., Perkin Trans. 2* **1999**, 493.